Inorganic Chemistry

Communication

pubs.acs.org/IC

# Slow Relaxation of the Magnetization in a 4,2-Wavelike $Fe^{III}_2Co^{II}$ Heterobimetallic Chain

Luminita Marilena Toma,[†] Catalina Ruiz-Pérez,[‡] Francesc Lloret,[†] and Miguel Julve*[,†]

[†]Departament de Química Inorgànica/Instituto de Ciencia Molecular, Facultat de Química de la Universitat de València, Polígono de la Coma s/n, 46980 Paterna, València, Spain

[‡]Laboratorio de Rayos X y Materiales Moleculares, Departamento de Física Fundamental II, Facultad de Física de la Universidad de La Laguna, Avda. Astrofísico Francisco Sánchez s/n, 38204 La Laguna, Tenerife, Spain

Supporting Information

**ABSTRACT:** The reaction of the low-spin iron(III) complex $[Fe(dmbpy)(CN)_4]^-$ (**1**) with fully solvated cobalt(II) ions affords the cyanide-bridged heterobimetallic chain $\{[Fe^{III}(dmbpy)(CN)_4]_2Co^{II}(H_2O)_2\}_n \cdot 4nH_2O$ (**2**), which exhibits intrachain ferromagnetic coupling and double slow relaxation of the magnetization.

Since the publication of the first example of a single-chain magnet (SCM) a decade ago,[1] this type of system has become very appealing in the field of molecular magnetism because of fundamental interest and potential applications in memory devices and quantum computation on the way toward the multifunctional magnetic molecular materials (MMMMs).[2−8] These systems, whose existence was first predicted by Glauber in 1963,[9] are magnetically isolated Ising chains with intrachain ferro- or antiferromagnetic coupling, which behave as magnets with hysteresis and slow relaxation of magnetization. It is not an easy task to fulfill these characteristics, as shown in a recent forum where the main preparative routes to obtain them have been outlined.[10] A molecular programmed bottom-up strategy that consists of using preformed cyanide-[3b,11] and oxamate-bearing[2,12] building blocks as ligands toward anisotropic transition metal ions has been developed in our group envisaging the rational design of SCMs. In this respect, the high-spin six-coordinate cobalt(II) ion was chosen because of its strong Ising-type anisotropy together with anionic paramagnetic cyanide- and oxamate-bearing mononuclear complexes that act as ligands. The steric effects caused by the presence of bulky substituents in the coordination sphere of the mononuclear precursor would minimize the interchain interactions between the adjacent bimetallic chains providing the magnetic isolation that is required to observe the SCM. Following this approach, we synthesized the low-spin iron(III) complex of formula $PPh_4[Fe^{III}(dmbpy)(CN)_4] \cdot 3H_2O$ (**1**) (dmbpy = 4,4′-dimethyl-2,2′-bipyridine and $PPh_4^+$ = tetraphenylphosphonium cation), and we used it as a ligand toward fully solvated cobalt(II) ions to afford the heterobimetallic chain $\{[Fe^{III}(dmbpy)(CN)_4]_2Co^{II}(H_2O)_2\}_n \cdot 4nH_2O$ (**2**). The preparation of **1** and **2**, their crystal structures and magnetic properties are reported herein (see Supporting Information).

The structure of **1** consists of mononuclear $[Fe^{III}(dmbpy)(CN)_4]^-$ anions (Figures S1 and S2 of the Supporting Information), $PPh_4^+$ cations, and crystallization water molecules. The iron atom in **1** is six-coordinated with two dmbpy−nitrogen and four cyanide−carbon atoms building a distorted octahedral coordination sphere. The values of the Fe−N [1.989(3) and 1.994(3) Å] and Fe−C [1.913(3)−1.955(4) Å] bond lengths and $\mu_{eff}$ at 300 K (ca. 2.28 $\mu_B$) agree with those reported for parent low-spin $[Fe^{III}(AA)(CN)_4]^-$ species (AA = bidentate nitrogen donor).[3b,11]

Compound **1** is present in **2** as a bis-monodentate ligand toward *trans*-diaquacobalt(II) units through two of its four cyanide−nitrogens in *cis* position to afford neutral cyanide-bridged 4,2-wavelike $\{[Fe^{III}(dmbpy)(CN)_4]_2Co^{II}(H_2O)_2\}$ chains, which run along the *a* axis (Figure 1a,b). Each iron atom in **2** exhibits the same surrounding as in **1** [Fe−C = 1.907(8)−1.956(11) Å and Fe−N = 1.974(6) and 1.978(6) Å]. The cobalt atom in **2** is also six-coordinated with four cyanide−nitrogen atoms [Co−N = 2.074(7) and 2.077(7) Å] and two water molecules in *trans* positions [Co−$O_w$ = 2.131(6) Å] building a distorted octahedral environment. The Co−N≡C fragments in **2** [167.9(8)° and 168.0(8)°] are significantly bent, whereas the Fe−C≡N angles for both terminal [179.5(8)° and 179.5(9)°] and bridging [175.7(8)° and 175.9(8)°] cyanide groups are much closer to the strict linearity. The values of the iron−cobalt separation through bridging cyanide in **2** are 5.058 Å. Within each chain, the roof-shaped $Fe_2Co_2$ tetranuclear motifs are located alternatively above and below the vector passing through the cobalt atoms (Figure 1b). The two water molecules coordinated to the adjacent cobalt atom in *cis* positions are interacting through hydrogen bonds with the two crystallization water molecules forming a roof shaped $(O_w)_4$ ring (Figure 1a,b), with an intraring $O_w\cdots O_w$ separation of 2.776(5) Å. A view of the crystal packing in the *bc* plane shows the occurrence of empty channels down the *a* axis, each one being formed by four neighboring bimetallic chains (Figure 1c). The average size of each hole is 7.0 × 7.0 Å.

The temperature dependence of $\chi_M T$ for **2** [$\chi_M$ being the magnetic susceptibility per $Fe^{III}_2Co^{II}$ unit] in the temperature range 1.9−300 K is shown in Figure S3 of the Supporting Information. At 300 K, $\chi_M T$ is 3.78 $cm^3\ mol^{-1}\ K$, a value which is well above the calculated one through the spin-only formula for one high-spin Co(II) ($S_{Co}$ = 3/2) and two low-spin Fe(III) ions ($S_{Fe}$ = 1/2) magnetically isolated (2.25 $cm^3\ mol^{-1}\ K$ with *g*

**Received:** November 9, 2011
**Published:** January 24, 2012

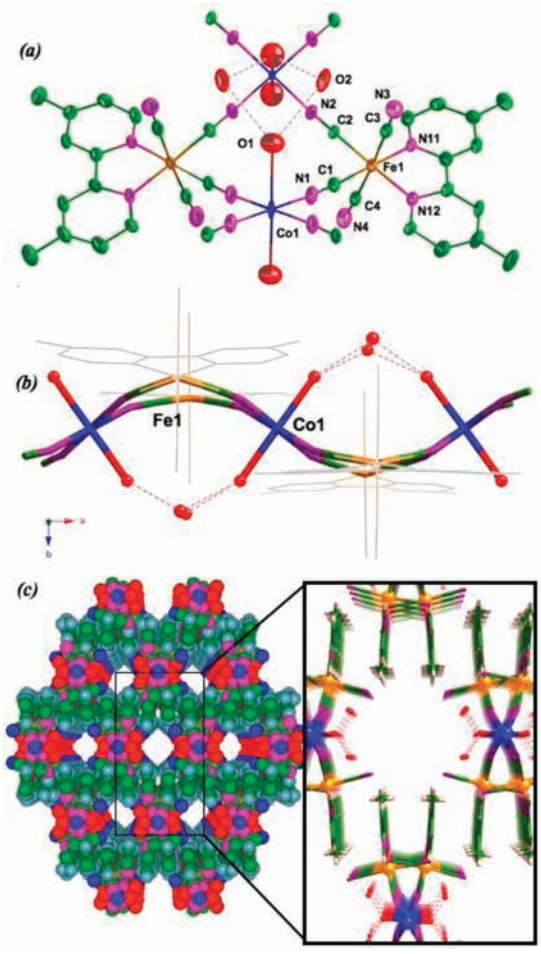


**Figure 1.** Perspective views of the structure of **2** showing: (a) atom numbering, (b) wavelike shape (hydrogen bonds are drawn as red dotted lines), and (c) supramolecular organization of the chains with a detail of the channels.

= 2.0) due to a significant orbital contribution of the two six-coordinated metal ions. Upon cooling, $\chi_M T$ smoothly increases until 20 K ($H$ = 1 T) and then sharply reaches a maximum value of 198.9 $cm^3\ mol^{-1}$ K at 4.0 K ($H$ = 100 G) indicating the presence of an intrachain ferromagnetic interaction. Finally, at lower temperatures, $\chi_M T$ decreases linearly with $T$, as the magnetization becomes field dependent. The magnetization versus $H$ plot at 2.0 K for **2** (inset of Figure S3 of the Supporting Information) supports also the ferromagnetic coupling: a sharp increase of the magnetization at very low magnetic fields with a value of 3.4 $\mu_B$ of the magnetization at 5 T, which is close to the calculated 4.0 $\mu_B$ [1 $\mu_B$ per $Fe^{III}$ and 2 $\mu_B$ per $Co^{II}$, assuming that only the ground Kramer's doublet of cobalt(II) is populated ($S_{Co}$ = 1/2 and $g_{Co}$ = 4.0) at low temperatures].[13] No hysteresis loop was observed for **2** at 2.0 K.

A frequency-dependent behavior is observed for the ac susceptibility measurements of **2** (Figure S4 of the Supporting Information). Best-fit data to an Arrhenius law ($\tau = \tau_0\ e^{-Ea/kT}$) leads to values of $\tau_0 = 4.3 \times 10^{-24}$ s (physically meaningless because its too small magnitude) and $E_a$ = 130.5 $cm^{-1}$ (the energy barrier quantifying the magnetization reversal); the slight curvature observed in the ln $\tau$ versus $1/T$ (Figure S5 of the Supporting Information) suggesting the occurrence of more than one potential energy barrier. The frequency shifts of $T_B$ (temperature of the $\chi''$ maximum in Figure S4 of the Supporting Information) obtained as (the so-called Mydosh parameter)[14a] give additional support for the presence of more than one relaxation process.[14b] A detailed analysis of the relaxation times and their dependence on the temperature is made using the phenomenological description of Cole−Cole,[15] the Argand diagrams at different temperatures being presented in Figure 2. Data fit through the Cole−Cole model considering

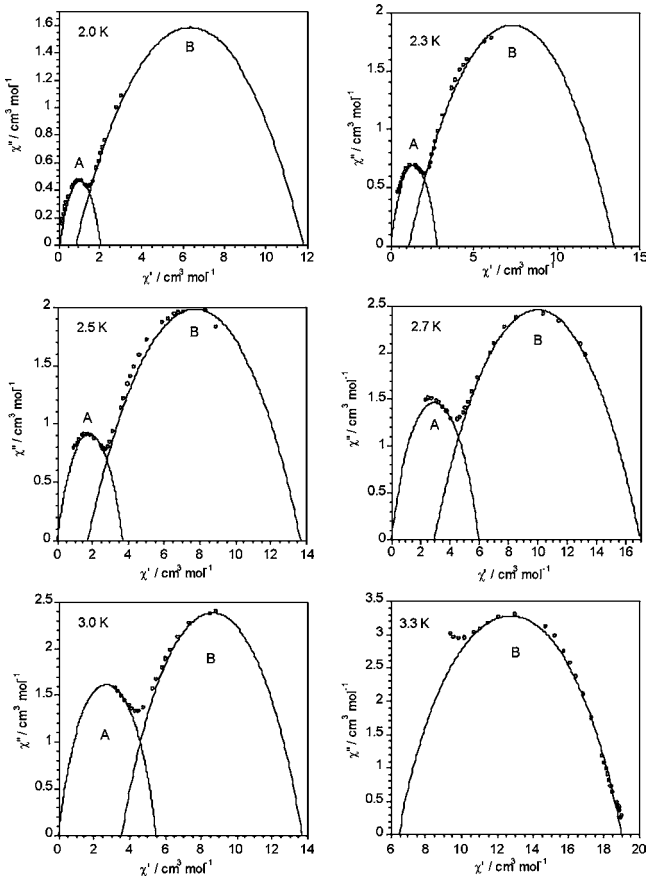


**Figure 2.** Argand diagrams for **2** at different temperatures. Solid lines are the least-squares fits obtained through a Cole−Cole model (see text).

each relaxation process (noted A and B) separately leads to values of $\alpha_A$ and $\alpha_B$ covering the ranges of 0.445 (2.0 K)−0.325 (3.0 K) and 0.641 (2.0 K)−0.386 (3.3 K), respectively (Table S3 of the Supporting Information), with $\alpha$ being a parameter that determines the width of the $\tau$ distribution. In general, values of $\alpha$ in the range of $0 < \alpha < 0.5$ are commonly attributed to interchain magnetic interactions, which in the present case are supported by the fact that the values of $\alpha$ increase as the temperature decreases. The values of $\tau$ at different temperatures for the two regimes (A and B) are obtained from the Cole−Cole model, and they follow the Arrhenius law (Figure S6 of the Supporting Information) characteristic of a thermally activated mechanism with $\tau_0 = 1.7 \times 10^{-8}$ (A) and $2.3 \times 10^{-11}$ s (B) and $E_a$ = 17.6 (A) and 42.1 $cm^{-1}$ (B). These values are within the range of those expected for a SCM. The B regime is the only one occurring at $T < 3.3$ K, whereas the A one becomes dominant at $T \leq 2.2$ K.

Given that the $\chi T$ product, under zero applied field, increases exponentially with decreasing temperature for an Ising-like


dx.doi.org/10.1021/ic202410t | Inorg. Chem. 2012, 51, 1216−1218

chain according to $\chi T \approx C \exp(\Delta\xi/kT)$ ($C$ being an effective Curie constant and $\Delta\xi$ the energy to create a domain wall in a chain),[10,16,17] we have examined the $\ln(\chi' T)$ against the $1/T$ plot of **2**, where $\chi'$ is the in-phase susceptibility at the lowest ac frequency studied ($H_{dc}$ = 0 and $H_{ac}$ = 1 G) (Figure S7 of the Supporting Information). The linear dependence observed in the temperature range of 4.4−16.0 K with a slope $\Delta\xi$ = 16.1 $cm^{-1}$ proved the 1D character of **2** and the presence of a significant anisotropy. One can see also that $\ln(\chi' T)$ reaches a maximum at 4.4 K and then decreases because of the blocking of $\chi'$.

The energy barrier in the Glauber's theory is $E_a = 2\Delta\xi$.[9] The value of this parameter obtained from the static properties [$\ln(\chi' T)$ vs $1/T$ in Figure S7 of the Supporting Information], $E_a = 2\Delta\xi$ = 32.2 $cm^{-1}$, is intermediate between those observed from the dynamics properties [$\ln(\tau)$ vs $1/T$ in Figure S6 of the Supporting Information], $E_a$ = 17.6 and 42.1 $cm^{-1}$ for the A and B regimes, respectively. Moreover, in the Ising limit, $\Delta\xi = 4|J| S_{Co} S_{Fe}$, and so, $E_a = 6|J|$ for $S_{Co}$ = 3/2 and $S_{Fe}$ = 1/2.[10,18] The values of $J$ obtained for the magnetic interaction in the pair $Fe^{III}$ (low-spin)($\mu$-CN)-$Co^{II}$ (high spin)[19] are in the range of 5−11 $cm^{-1}$. Consequently, an energy barrier spanning in the range of 30 − 60 $cm^{-1}$ would be expected, and the value for this barrier in **2** would lie within this range. Finally, it deserves to be noted that the occurrence of two different relaxation processes describing two independent semicircles in the Argand plot was also observed recently in an oxamato-bridged $Cu^{II}Co^{II}$ SCM.[2b] In the present case, we have checked that this phenomenology is an intrinsic property of the product by controlling the purity and avoiding partial dehydration in **2**.

## ■ ASSOCIATED CONTENT

### Supporting Information

Structural drawings of **1** (Figures S1 and S2); thermal dependence of $\chi_M T$ (inset shows the $M$ vs $H$ plot at 2.0 K) (Figure S3) and of the real ($\chi_M'$) and imaginary ($\chi_M''$) parts of the ac susceptibility (Figure S4), and ln $\tau$ (Figures S5 and S6) and ln ($\chi_M' T$) against $1/T$ (Figure S7) for **2**; CCDC 830594 (**1**) and 830595 (**2**) contain the X-ray crystallographic data as cif files. This material is available free of charge via the Internet at http://pubs.acs.org.

## ■ AUTHOR INFORMATION

### Corresponding Author

*E-mail: miguel.julve@uv.es.

## ■ ACKNOWLEDGMENTS

This work was supported by the Ministerio Español de Ciencia e Innovación (Projects CTQ2010-15364, MAT2010-19681, CSD-2007-00010, and CSD2006-00015) and the Generalitat Valenciana (Project PROMETEO/2009/108).

## ■ REFERENCES

(1) Caneschi, A.; Gatteschi, D.; Lalioti, N.; San Gregorio, C.; Sessoli, R.; Venturi, G.; Vindigni, A.; Rettori, A.; Pini, M. G.; Novak, M. A. *Angew. Chem., Int. Ed.* **2001**, *40*, 1760.

(2) (a) Dul, M. C.; Pardo, E.; Lescouëzec, R.; Journaux, Y.; Ferrando-Soria, J.; Ruz-García, R.; Cano, J.; Julve, M.; Lloret, F.; Cangussu, D.; Pereira, C. L. M.; Stumpf, H. O.; Pasán, J.; Ruiz-Pérez, C. *Coord. Chem. Rev.* **2010**, *254*, 2281. (b) Ferrando-Soria, J.; Pardo, E.; Ruiz-García, R.; Cano, J.; Lloret, F.; Julve, M.; Journaux, Y.; Pasán, J.; Ruiz-Pérez, C. *Chem.—Eur. J.* **2011**, *17*, 2176. (c) Pardo, E.; Train, C.; Lescouëzec, R.; Journaux, Y.; Pasán, J.; Ruiz-Pérez, C.; Delgado, F. S.; Ruiz-García, R.; Lloret, F.; Paulsen, C. *Chem. Commun.* **2010**, *46*, 2010.

(3) (a) Liu, T.; Zhang, Y. J.; Kanegawa, S.; Sato, O. *J. Am. Chem. Soc.* **2010**, *132*, 8250. (b) Toma, L. M.; Lescouëzec, R.; Pasán, J.; Ruiz-Pérez, C.; Vaissermann, J.; Cano, J.; Carrasco, R.; Wernsdorfer, W.; Julve, M.; Lloret, F. *J. Am. Chem. Soc.* **2006**, *128*, 4842.

(4) (a) Sato, O. *Acc. Chem. Res.* **2003**, *36*, 9692. (b) Arimoto, Y.; Ohkoshi, S.; Zhong, Z. J.; Seino, H.; Mizobe, Y.; Hashimoto, K. *J. Am. Chem. Soc.* **2003**, *125*, 9240.

(5) (a) Niel, V.; Thompson, A. L.; Muñoz, M. C.; Galet, A.; Goeta, A. E; Real, J. A. *Angew. Chem., Int. Ed.* **2003**, *42*, 3760. (b) Takahashi, K.; Kawakami, V.; Gu, Z.; Einaga, Y.; Fujishima, A.; Sato, O. *Chem. Commun.* **2003**, 2374. (c) Halder, G. J.; Kepert, C. J.; Moubaraki, B.; Murray, K. S.; Cashion, J. D. *Science* **2002**, *298*, 1762.

(6) Coronado, E.; Day, P. *Chem. Rev.* **2004**, *104*, 5419.

(7) (a) Inoue, K.; Kikuchi, K.; Ohba, M.; Okawa, H. *Angew. Chim. Int. Ed.* **2003**, *42*, 4709. (b) Coronado, E.; Galán-Mascarós, J. R.; Gómez-García, C. J.; Martínez-Agudo, J. M. *Inorg. Chem.* **2001**, *40*, 113. (c) Mamula, O.; von Zelewsky, A.; Bark, T.; Stoeckli-Evans, H.; Neels, A.; Bernardelli, G. *Chem.—Eur. J.* **2000**, *6*, 3575.

(8) Train, C.; Gheorghe, R.; Krstic, V.; Chamoreau, L. M.; Ovanesyan, N. S.; Rikken, G. L. J. A.; Gruselle, V.; Verdaguer, M. *Nat. Mater.* **2008**, *9*, 729.

(9) Glauber, R. J. *J. Math. Phys.* **1963**, *4*, 294.

(10) Miyasaka, H.; Julve, M.; Yamashita, M.; Clérac, R. *Inorg. Chem.* **2009**, *48*, 3420.

(11) Lescouëzec, R.; Toma, L. M.; Vaissermann, J.; Verdaguer, M.; Delgado, F. S.; Ruiz-Pérez, C.; Lloret, F.; Julve, M. *Coord. Chem. Rev.* **2005**, *249*, 2691.

(12) Pardo, E.; Ruiz-García, R.; Cano, J.; Ottenwaelder, X.; Lescouëzec, R.; Journaux, Y.; Lloret, F.; Julve, M. *Dalton Trans.* **2008**, 2780.

(13) (a) Lloret, F.; Julve, M.; Cano, V; Ruiz-García, R.; Pardo, E. *Inorg. Chim. Acta* **2008**, *361*, 3432.

(14) (a) Mydosh, J. A. In *Spin Glasses: An Experimental Introduction*; Taylor and Francis: London, 1993. (b) These values fall between those of a pure superparamagnet ($F \approx 0.3-0.15$) and of spin glasses ($F \approx 0.01-0.001$).

(15) Cole, K. S.; Cole, R. H. *J. Chem. Phys.* **1941**, *9*, 341.

(16) Coulon, C.; Miyasaka, H.; Clérac, R. *Struct. Bonding (Berlin)* **2006**, *122*, 163.

(17) (a) Loveluck, J. M.; Lovesey, S. W.; Aubrey, S. *J. Phys. C: Solid State Phys.* **1975**, *8*, 3841. (b) Nakamura, K.; Sasada, T. *J. Phys. C: Solid State Phys.* **1978**, *11*, 331.

(18) Using a spin Hamiltonian as $\boldsymbol{H} = -J\boldsymbol{S}_i \cdot \boldsymbol{S}_{i+1}$ and taking into account that each Co(II) ion interacts with four Fe(III) centers in **2**.

(19) Pardo, M.; Verdaguer, M.; Herson, P.; Rousselière, H.; Cano, J.; Julve, M.; Lloret, F.; Lescouëzec, R. *Inorg. Chem.* **2011**, *50*, 6250.